SPE 112239

Short-Term Production Optimization by Automated Adaptive Modeling and Control

Ankur Awasthi, University of Houston; Sathish Sankaran, SPE, Halliburton-Landmark; Michael Nikolaou, SPE, University of Houston; and Luigi Saputelli, SPE, and Gerardo Mijares, SPE, Halliburton-Landmark

This paper was prepared for presentation at the 2008 SPE Intelligent Energy Conference and Exhibition held in Amsterdam, The Netherlands, 25–27 February 2008.

Abstract

Short-term production optimization relying on model-based predictions over a short period (weeks to months) requires the use a near-borehole reservoir model. Such a model is usually developed and validated through standard well testing. Standard well testing has to be repeated periodically, with related loss of production. Production losses may be reduced by prolonging the interval between tests, but that may compromise the quality of information about reservoir properties, such as skin (or productivity index), which would ultimately compromise production as well. Therefore, a need exists for a methodology that maximizes both reservoir information and production simultaneously. Because these two tasks are inherently contradictory, a compromise has to be found. In this work we propose a methodology that combines well testing and production in an optimal way, resulting in overall production optimization. This methodology relies on a short-term moving-horizon optimization of an objective function that includes terms referring both to the quality of reservoir information and to production net present value. Reservoir information is captured by empirical (proxy) models that are built adaptively on-line as a result of optimal perturbations of production rates and recording of dynamic responses of related bottomhole pressures. Besides, the entire workflow can be automated. Simulations are presented that illustrate the mechanics and value of the proposed methodology.

Introduction

The oil and gas industry is facing remarkable challenges to maximize profitability in a dynamic and uncertain environment while satisfying a variety of constraints. Current practices of production optimization involve combining mathematical models, field data and experience to make decisions about optimal production scenarios. In recent literature, a number of proxy modeling techniques [1-10] have been proposed where the output variables (oil recovery factor, multiphase flow rates etc.) are modeled as a function of the input variables. However, most of these methods focus on data-driven approaches such as response surface techniques based on regression, interpolation, neural network etc. These methods are relatively easy to setup and capture the nonlinear effects in the training data set. However, reservoir phenomena unseen in the past (e.g., water breakthrough) or operating regimes that lie outside the range of training data set are not adequately predicted by such models. Further, most proxy modeling approaches used in production optimization actually model the reservoir simulator outputs and are seldom validated against real field data.

The authors of this paper have developed a parametric modeling methodology for Real-Time Production Optimization (RTPO) strategy [11, 12]. Since the parametric model structure is derived from reservoir physics, it is expected that the model will be suitable to extrapolate outside the training data set. A feasible approach to continuous model updating and short-term forecasting using this approach was presented in [13].

Though continuous field data (production/injection rates and pressure) is used in the proposed approach to periodically update the parametric model, the production rates are often not measured but estimated through production allocation. In many oil and gas assets, commingled production from multiple wells (or even zones in a stacked reservoir) is a common practice, where flow rate measurements are taken downstream of the mixing point. This introduces uncertainties in determining the individual production rates of each well (or zone) in the reservoir. The accuracy and quality of allocated production data can significantly impact history matching of reservoir models, estimation of remaining reserves, production optimization (short-term and long-term) and reservoir management decisions. Regulatory reporting requirements address this problem by mandating periodic surface well tests, where an individual well (or sometimes zone) is routed to a test separator and multiphase flow rates are measured without the intervention of other wells in the field. An allocation factor is computed for each well (or zone) based on its relative contribution to the total production. However, this procedure may require rerouting or shutting down other wells (or zones) in the field for the duration of the test. Thus, it is often associated with increased operating costs or deferred production. Additionally, it is assumed that the well does not change behavior in between the well tests. Error-spreading is another common drawback of this approach, especially when pressure information is used without reconciling with known downtime events as described in [14, 15].

In this paper, we focus on the methodology to update the parametric reservoir model with relevant field data whenever it becomes available – namely well test information in addition to daily production data. This information is used in a production allocation workflow to estimate the well (and zonal) rates from regular field data in a commingled production scenario. A brief overview of the modeling framework and reservoir parametric modeling methodology is presented followed by a discussion of the least squares optimization problem formulation that is used to back allocate the rates. This reduces the distribution of allocation errors to all wells (or zones) – either spread evenly or weighted according to the last observed well (or zone) potential, as observed in conventional practice. Continuous reconciliation with field data and use of reservoir physics can also potentially reduce the number of surface well tests conducted significantly. The following sections describe the results of the proposed approach using two case studies and sensitivity analysis on selected reservoir parameters.

Modeling Framework

Over the years, reservoir simulators have been used for reservoir management purposes. With advances smart well technologies including downhole sensors and control elements, it is now possible to measure and analyze more and more data from the field. This increase in available data further enables development of advanced reservoir simulation strategies for improved reservoir characterization. While such large and complex models result in better long-term predictions and overall field management, these models are often achieved at the cost of high computation time. On the other hand, such model needs to be continuously updated to ensure accurate short-term predictions necessary for daily production optimization.

In the past few years, various data-driven approaches for real-time decision making have been proposed, such as neural networks [16], wavelets [17], optimal control [18] etc. However, most of these approaches are purely data driven, do not consider the underlying physics and cannot be validated or updated based on plant measurements. The proposed modeling approach addresses this gap to make more accurate short-term predictions based on the real-time field data [12, 13]. It is briefly described in the following section.

Short-term Parametric Model. From first principles (conservation of mass) and constitutive equations (Darcy's law, compressibility equations, and capillary pressure equations) — after discretization of derivatives with respect to the spatial co-ordinates — one can get a reservoir model in vector-matrix form as follows:

$$\hat{\mathbf{B}}\frac{d\hat{\mathbf{p}}}{dt} = \hat{\mathbf{T}}_m\hat{\mathbf{p}}(t) - \mathbf{T}_h\mathbf{h} + \hat{\mathbf{q}}(t) \tag{1}$$

where $\hat{\mathbf{p}}_{i,j,k}$ contains values of block oil pressure, water saturation and gas saturation respectively, sufficient to complete the reservoir description at all discretization points (grid blocks) indexed by $[i, j, k]$. The vector $\hat{\mathbf{q}}$ contains all external fluid flows, using the convention that these external fluid flows are negative at production points, positive at injection points and zero at all other points. A more detailed discussion and related references are offered in [13].

In our previous work [12], we have shown that the time dependence of the matrices in Eq. (1) is relatively weak for short-term time scales. Therefore, a simplified input-output model of the reservoir can be formulated using a state-space structure [19, 20], as follows:

$$\begin{aligned}\frac{d\mathbf{x}}{dt} &= \mathbf{Ax}(t) + \mathbf{Bu}(t)\\ \mathbf{y}(t) &= \mathbf{Cx}(t) + \mathbf{Du}(t)\end{aligned} \tag{2}$$

where the vector $\mathbf{x}$ comprises the states of the system, namely the values of p_o, S_w and S_g at all discretization points in the reservoir; the vector $\mathbf{y}$ captures the measured outputs, and the vector $\mathbf{u}$ captures the effect of inputs.

The inputs and outputs can be chosen relevant to the workflow application where the model will be used. For example, in production foreacasting, the relevant inputs and outputs are the bottomhole pressures (or production choke settings) and the multiphase production rates at the producer grid blocks respectively [13]. Similarly, when using such a model for multi-scale resolution of the production optimization problem, injection rates can be included as inputs in addition to bottomhole pressures, where it may be required to estimate the optimum injection rates by maximizing total profit over a period of time [21].

However, in all such cases the inherent assumption is the availability of individual production rates, which may or may not be available in a multi-layered reservoir where the rates need to be allocated on a zonal (per layer) basis for each well.

Rate Allocation during Commingled Production

Production allocation is particularly vital where multiple wells (and often layers) are present in a reservoir, where the most economical operating practice is to commingle the production from all the wells (and layers). Traditional operating practice is to isolate each well (or zone) during well testing or otherwise and estimate the potential at which each well (or zone) can produce. The well (or zonal) rates are then allocated over time assuming the well (or zone) can produce at its last estimated potential until new individual rates are measured again. A single well (or zonal) test requires dedicating the available resources (flowlines, manifolds, separator etc.) to the tested well (or zone), which requires re-routing of the remaining wells (and zones) in the field, often resulting in production losses. Futher, the level of instrumentation in each well typically allows surface control of wells but this may be difficult and often impossible for multiple producing zones in each well.

In practice, such a rate-allocation exercise is often demanded by regulatory authorities. In addition, such well testing can provide valuable information for optimum reservoir developments and production optimization.

Such conventional allocation practice relies on frequent well (or zonal) tests and the assumption that there isn't any significant change in the reservoir properties during this interval, which is hardly the case. The following example demonstrates how the parametric model presented in the previous section can be validated as a viable model to make accurate short-term predictions when such measurements become available.

Model Validation. The problem of allocating production rates on a well (or zonal) basis assumes that the field measurements available, are the total production rates and pressure at the separator, choke positions and wellhead (and maybe bottomhole pressures). The bottomhole pressures are increasingly made available with downhole sensors, as illustrated in Figure 1.

The choice of inputs and outputs is reversed for the production allocation workflow, as compared to the previously discussed workflows [13, 21] – namely production forecasting and production optimization; and so we refer to this as the "*inverse model approach*". In order to validate the model for short-term production, we use the two layered reservoir with one producer, one injector as shown in Figure 2. Both the wells (injector and producer) are perforated at each of the two layers. The reservoir has a (upper) low-permeability layer and a (lower) high-permeability layer, separated by an impermeable layer. The difference in the permeability values (ratio 1:2.5) between the two layers makes a pre-defined or rule-based allocation difficult and often inconsistent.

Simulated production data from a full-physics reservoir model is used to identify the "*inverse model*". The oil production rates from the two zones are the measured inputs; and the bottomhole pressures are the measured outputs, thus making it a 2×2 multivariable input-output model. The evolution of inputs and outputs for both the zones, i.e., upper Zone-1 and lower Zone-2 are plotted in Figure 3 over a period of 2000 days. The daily identified linear models are used with the corresponding input values (zonal rates) to make 7-day-ahead (Figure 4) and 30-day-ahead (Figure 5) predictions of the resulting bottomhole pressures of the two zones.

The average errors (for both zones) between the actual (solid line) and the predicted value (dotted line) for the 7-day-ahead and 30-day-ahead predictions are 0.7% and 10% respectively. The predicted pressures match the actual values better for the 7-day-ahead case as expected, while the accuracy of the match deteriorates for long-term (30-day-ahead) predictions. The increase in this error can be attributed to the cumulative errors involved in estimating the average values in the future. It should be noted that the predictions compared here only account for the early days of the reservoir, i.e., when water has not reached any of the producer zones.

The modeling approach used here focuses on predicting bottomhole pressures, assuming the allocation rates are known, which establishes a parametric model between the two and results in predictions of reasonable accuracy (<10%). The same strategy can be extended to ensure optimal zonal allocations using an optimization procedure as discussed in the following section.

Production Allocation: A Least Squares Optimization

In this work, bottomhole pressure data is used to allocate production rates to their respective zones and wells using the "*inverse model*" approach developed earlier, while ensuring that the total measured production (Q_T) is honoured. As the pressure data ($\mathbf{p}_{wf}^m$) and total rate (Q_T) are continuously measured, the optimal zonal rates are calculated by minimizing the following least squares objective function:

$$\min_{\mathbf{u}} \sum_{k=1}^{P} \sum_{i=1}^{N_z} (\hat{y}_{i,j} - y_{i,k}^m)^2 \tag{3}$$

where $y_{i,k}^m$ is the measured bottomhole pressure of zone i at time k, $\hat{y}_{i,k}$ is the predicted bottomhole pressure of zone i at time k, $\mathbf{u}$ is the vector of zonal production rates, N_z is the total number of zones and P is the prediction horizon.

The least squares optimization is solved over a prediction horizon P (days), if an allocation is done on a fixed schedule. However, the value of using such a methodology is when solving it in real-time (relevant time scale), e.g., daily, where the allocation routine will be run as soon as the downhole pressure and surface rate measurements become available. To account for the surface rate measurement, the optimization problem is subject to the following total rate constraint over the prediction horizon P:

$$\sum_{i=1}^{N_z} u_{i,k} = Q_{T,k}, \quad k = 1, 2, ...P \tag{4}$$

where $u_{i,k}$ is the zonal production rate for zone i at time k and $Q_{T,k}$ is the total production rate at time k measured at the separator. The optimization problem in Eq. (3) with the constraint in Eq. (4) can be simplified as the following convex optimization problem (see Appendix A):

$$\begin{aligned} &\min_{\mathbf{u}} \mathbf{u}^T \mathbf{H} \mathbf{u} + \mathbf{u}^T \mathbf{f} \\ &\mathbf{A}_e \mathbf{u} = \mathbf{b}_e \end{aligned} \tag{5}$$

The rate-allocation workflow is illustrated in Figure 6 where the optimal allocation rates are calculated based on the least squares optimization and the constraint described in Eq. (3) - (4). It is assumed that the well test information (less frequently) can also be incorporated into the workflow whenever available. The first step in the process is to start from an initial model that can be obtained through well tests by isolating the respective zones. Once such a model (described by the state-space form in Eq. (2)) is established, individual zonal rates are estimated using the new bottomhole pressure and surface rate measurements and solving the least squares optimization in Eq. (3) subject to the total constraint in Eq. (4). The process is repeated over a period of time using the last available model until a new model is available, i.e., when a new well test or zonal test is performed. Such an update can be infrequent and can vary for different wells and zones. On the other hand, a structured model update procedure is important and needs to be consistent with the optimization problem.

Model Updating

As shown in Figure 6, the optimal allocated rates are calculated until new measurements are available, i.e., when the model needs to be updated and new optimal rates are calculated. In practice, individual zonal rates can be measured by shutting-in the zone using downhole flow control valves during scheduled well (or zonal) tests. Once individual well or zonal rates are acquired, the corresponding well or zone model needs to be updated with higher emphasis placed on recent data.

Our previous discussion of identifying parametric models, as shown in Eq. (2), can be extended to the following state-space model (discrete time domain) for each zone:

$$\begin{aligned}\mathbf{x}_{k+1} &= \mathbf{A}_i \mathbf{x}_k + \mathbf{B}_i \mathbf{u}^i_k \\ \hat{\mathbf{y}}^i_{k+1} &= \mathbf{C}_i \mathbf{x}_{k+1} + \mathbf{D}_i \mathbf{u}^i_{k+1}\end{aligned} \tag{6}$$

where $\mathbf{A}_i, \mathbf{B}_i, \mathbf{C}_i, \mathbf{D}_i$ are the system matrices for the i^{th} zone. The separate linear models for all the zones (and wells), i.e., $i = 1, 2, ..., N_z$ can be combined in a compact form (see Appendix B):

$$\begin{aligned}\mathbf{x}_{k+1} &= \mathbf{A}\mathbf{x}_k + \mathbf{B}\mathbf{u}_k \\ \hat{\mathbf{y}}_{k+1} &= \mathbf{C}\mathbf{x}_{k+1} + \mathbf{D}\mathbf{u}_{k+1}\end{aligned} \tag{7}$$

where the state matrix $\mathbf{A}$ is in the block diagonal form capturing the internal dynamics of the system:

$$\mathbf{A} = \begin{pmatrix} \mathbf{A}_1 & & & & \\ & \mathbf{A}_2 & & & \\ & & \cdot & & \\ & & & \cdot & \\ & & & & \mathbf{A}_{N_z} \end{pmatrix} \tag{8}$$

The structure of this compact parametric model provides the flexibility to update each of the model matrices ($\mathbf{A}_i$) individually, whenever required. For example, a well (or zone) scheduled to be tested at the beginning of the month can be updated separately and another at the middle of the month.

Results

The two examples discussed here illustrate the optimal production allocation approach on a small reservoir with a few wells. We used a simulated model to generate daily data, assuming:

- Average daily bottomhole pressures are known
- Total rate (Q_T) is known
- Initial model was estimated using the zonal rates measured by isolating individual zones

Case Study I. This case study involves a two-layered (two zones) reservoir with one injector and one producer in a line drive problem (one-quarter 5-spot configuration [21]) as shown in Figure 2. The production plan as shown in Figure 3 involves commingling the production from both the zones using common production tubing equipped with permanent downhole pressure gauges. Both the injector and the producer are perforated at each of the two zones and water was injected in both the zones for pressure maintenance. The main challenge here is to allocate rates for the two zones with different permeability values (ratio 1:2.5).

The model was updated as the well test is performed at the end of each month, and each zone is tested separately. The parametric model for each zone will then be updated every 30 days and the allocation exercise was repeated over a period of 1600 days, well after water breakthrough has occurred in both zones. Figure 7 shows comparison between the optimal allocated (oil) rates (dotted line) and the actual rates (solid line) for both zones (Zone-1 and Zone-2). The accuracy of the estimated allocated rates can be determined based on the following per-cent error calculated as:

$$\%\mathrm{error}_{\mathrm{i}} = 1 - \frac{\left\| \hat{\mathbf{y}}_i - \mathbf{y}_i \right\|_2}{\left\| \mathbf{y}_i - \bar{\mathbf{y}}_i \right\|_2} \tag{9}$$

where $\mathbf{y}_i$ is the time vector of the i-th measured output and $\hat{\mathbf{y}}_i$ is the time vector of the i-th predicted output.

The total allocation error calculated using Eq. (9) is 5.9% showing that the optimization problem can be solved with reasonable accuracy. Also, the total calculated rate matched up with the measured rate Q_T ensuring feasibility of the optimization problem.

Figure 8 shows comparison between predicted bottomhole pressures during optimization (dotted line) and the measured values (solid line), showing an 8% error. The linear parametric model used here may not be perfect; however it captures the reservoir dynamic behavior that is important for the rate-allocation strategy.

Case Study II. The rate-allocation optimization in Case Study I was performed for a single well with multiple zones. However, the problem is more challenging in a practical scenario with multiple wells and multiple zones as shown in the schematic in Figure 9. The two symmetrically distributed producers (Well-1 and Well-2) are connected to the same separator through the surface network where the total rate is measured and reported. All the wells, i.e., both producers and injectors are perforated at each of the two zones.

The wells are equipped with smart completions with remotely activated valves and downhole sensors. We adopt the model update strategy where a well test for the two producers is scheduled such that Well-1 (both zones - Zone-1 and Zone-2) is tested at the end of each month while Well-2 (both zones - Zone-1 and Zone-2) is tested at the middle (15^{th}) of every month. The two zones have distinct permeabilities, i.e., upper zone (Zone-1) equals 40 md and lower zone (Zone-2) equals 100 md. The optimization routine is solved continuously over a period of 1600 days.

The total measured rate is back allocated to the two producers (Well-1 and Well-2) and then to their respective zones (Zone-1 and Zone-2) as shown in Figure 10. The calculated rates (dotted line) match well with the actual (solid line) values and can be gauged based on the average allocated error of 10% calculated using Eq. (9). As shown in Figure 10 (lower right) the high permeability zone i.e. Zone-2 of Well-2 was intermediately shut-in (e.g., 1000 days) as a part of the production plan and the model was able to adapt to the field plan and allocate rates appropriately. However, it should be noted that to ensure proper allocation the model needs to be updated accordingly.

While the optimization strategy is implemented, the parametric model continuously predicts the output while minimizing the objective function in Eq. (3) at each time step. As shown in Figure 11 the model predicts the bottomhole pressures (dotted line) with a prediction error of 6% when compared to the measured bottomhole pressure (solid line) values. The accuracy of the predictions and the allocated errors indicates that such an allocation optimization can be generalized to multiple well and multiple zone reservoirs.

Sensitivity Analysis

The sensitivity of the proposed optimization algorithm was analyzed with respect to different operating conditions. For example, here we consider different reservoir characterizations, i.e., with different permeability ratios for the two-layered reservoir described in Figure 2 while the production plan implemented is the same as used in Case Study I. Figure 12 shows a comparison between different fields with different permeability ratios; i.e., k_2 / k_1 where k_1 is the permeability of the low permeability zone, and k_2 is the permeability of the high permeability zone. The cumulative allocation errors are plotted at each time step when the model was updated, i.e., at the end of every month. While all the scenarios shown in Figure 12 are within reasonable accuracy, the permeability ratio of 5 (diamond marker) has the minimum allocation error.

Figure 13 shows the cumulative prediction errors during the optimization process, where the model is updated after 30 days. Similar to the allocation errors, the prediction errors are within reasonable accuracy; and the field with permeability ratio of 5 (diamond marker) has the minimum error. The reason for the least error corresponding to the field with permeability ratio of 5 compared to other fields can be attributed to using similar production plan and field constraints even when applying them to entirely different fields, which requires further studies.

Conclusions

In this work, an optimization-based rate-allocation method was developed and successfully applied to two case studies with smart wells. The problem is presented as a convex optimization problem using a parametric model to make bottomhole pressure predictions. A linear constraint on the individual zonal rates was implemented, in order to satisfy the total measured rate. Also, a model update strategy is applied to ensure the model is kept up-to-date, as soon as any information on the respective well (or zone) is reported.

The allocated production rates are best estimates of the respective zonal rates, given the uncertainty of the reservoir and the well parameters. The field examples illustrated that the proposed rate-allocation method can estimate rates that are reasonably accurate e.g., 6% for case study I and 10% for case study II. The predicted bottomhole pressures for the two case studies were consistent with the measured values with error values of 8% and 6% respectively. Also, a sensitivity analysis provided valuable information about the proposed method when applied to different fields, resulting in consistent rate-allocations. The method proposed here accounts for oil production and can be refined to account for water production after water breakthrough.

Acknowledgements

The authors would like to thank Halliburton and University of Houston for permission to publish this work. The authors acknowledge the following software contributions: VIP reservoir simulator from Halliburton and MATLAB.

Nomenclature

Boldface uppercase: Matrix
Boldface lowercase: Vector

q : Flow rate
S : Saturation
P : Prediction horizon
p_{wf}^{m} : Measured bottomhole pressure
Q_T : Total production rate
$\hat{\mathbf{y}}_i$: i-th predicted output vector
$\mathbf{u}$: Input vector
$\mathbf{y}$: Output vector
$\mathbf{x}$: State vector
$\hat{\mathbf{p}}$: Pressure vector
$\mathbf{A}$: Matrix determining system dynamics
$\mathbf{B}$: Matrix determining input effects
$\mathbf{C}$: Matrix determining system outputs
$\hat{\mathbf{T}}_m$: Transmissibility matrix
$\hat{\mathbf{T}}_h$: Transmissibility matrix for gravity driven flow
$\hat{\mathbf{B}}$: Storage matrix

Abbreviations
BHP: Bottomhole pressure
MPC: Model Predictive Control

Subscripts
o : Oil
w: Water
g: Gas
inj: Injection
k: Current time
m: Mobility term
h: Gravity term
i,j,k: Block indexes

References

1. Chu, C., "Prediction of Steamflood Performance in Heavy-Oil Reservoirs Using Correlations Developed by Factorial Design Method". SPE Paper No. 20020. Presented at the *SPE California Regional Meeting*, Ventura, CA, 1990
2. Corre, P., P. Thore, V. de Feraudy, and G. Vincent, "Integrated Uncertainty Assessment For Project Evaluation and Risk Analysis". SPE Paper No. 65205. Presented at the *European Petroleum Conference*, Paris, France, 2000
3. Damsleth, E., A. Hage, and R. Volden, *Maximum Information at Minimum Cost: A North Sea Field Development Study With an Experimental Design.* Journal of Petroleum Technology, 1992. **44**: p. 1350-1356.
4. Dejean, J.P. and G. Blanc, "Managing Uncertainties on Productions Using Integrated Statistical Methods". SPE Paper No. 56696. Presented at the *Annual Technical Conference and Exhibition*, Houston, TX, USA, 1999

5. Egeland, T.e.a., "Designing Better Decisions". SPE Paper No. 24275. Presented at the *European Petroleum Computer Conference*, Stavanger, 1992
6. Eide, A.L., L. Holden, E. Reiso, and S.I. Aanaonsen, "Automatic History Matching by Use of Response Surfaces and Experimental Design". Presented at the *4th European Conference on the Mathematics of Oil Recovery*, Røros, Norway, 1994
7. Friedmann, F., A. Chawathé, and D.K. Larue, *Assessing Uncertainty in Channelized Reservoir Using Experimental Designs.* SPE Reservoir Evaluation & Engineering, 2003. **6**: p. 264-274.
8. Güyagüler, B. and R.N. Horne, "Uncertainty Assessment of Well-Placement Optimization". SPE Paper No. 71625. Presented at the *Annual Technical Conference and Exhibition*, New Orleans, Louisiana, 2001
9. Landa, J.L. and B. Güyagüler, "A Methodology for History Matching and the Assessment of Uncertainties Associated with Flow Prediction". SPE Paper No. 84465. Presented at the *Annual Technical Conference and Exhibition*, Denver, Colorado, 2003
10. Manceau, E., M. Mezghani, Zabalza-Mezghani, and F. Roggero, "Combination of Experimental Design and Joint Modeling Methods for Quantifying the Risk Associated With Deterministic and Stochastic Uncertainties – An Integrated Test Study". SPE Paper No. 71620. Presented at the *Annual Technical Conference and Exhibition*, New Orleans, Louisiana, 2001
11. Nikolaou, M., A.S. Cullick, and L. Saputelli, *Production Optimization - A Moving Horizon Approach.* SPE 99358, 2006.
12. Nikolaou, M., A.S. Cullick, L. Saputelli, G. Mijares, and S. Sankaran, "A Consistent Approach toward Reservoir Simulation at Different Time Scales". SPE Paper No. 99451. Presented at the *Intelligent Energy Conference and Exhibition*, Amsterdam, Netherlands, 2006
13. Awasthi, A., S. Sankaran, M. Nikolaou, L. Saputelli, and G. Mijares, "Closing the Gap between Reservoir Simulation and Production Optimization". SPE Paper No. 107463. Presented at the *Digital Energy Conference and Exhibition*, Houston, TX, USA, 2007
14. Gũyagũler, B. and T. Byer, "A New Production Allocation Optimization Framework". SPE Paper No. 105200. Presented at the *SPE Reservoir Simulation Symposium*, Houston, Texas, USA, 2007
15. McCracken, M. and D. Chorneyko, "Rate Allocation Using Permanent Downhole Pressures". SPE Paper No. 103222. Presented at the *SPE Annual Technical Conference*, San Antonio, Texas, USA, 2006
16. Ternyik, J., H. Bilgesu, S. Mohaghegh, and D. Rose, *Virtual Measurement in Pipes, Part I: Flowing Bottom Hole Pressure under Multi-phase flow and inclined wellbore conditions.* SPE 30975, 1995.
17. Jansen, J.D. and M.G. Kelkar, "Application of Wavelets to production data in describing Inter-well relationships". SPE Paper No. 38876. Presented at the *ATCE*, San Antonio, Texas, 1997
18. Brouwer, D.R. and J.D. Jansen, *Dynamic Optimization of Waterflooding With Smart Wells Using Optimal Control Theory.* SPE Journal, 2004. **9**(4): p. 391-402.
19. Brogan, W.L., *Modern Control Theory*. 3rd ed, ed. P. Hall. 1991.
20. Kailath, T., *Linear Systems*, ed. P.-. Hall. 1980.
21. Awasthi, A., S. Sankaran, M. Nikolaou, L. Saputelli, and G. Mijares, "Meeting the Challenges of Real Time Production Optimization - A Parametric Model-based Approach". SPE Paper No. 111853. Presented at the *Intelligent Energy Conference and Exhibition*, Amsterdam, Netherlands, 2008

Figures

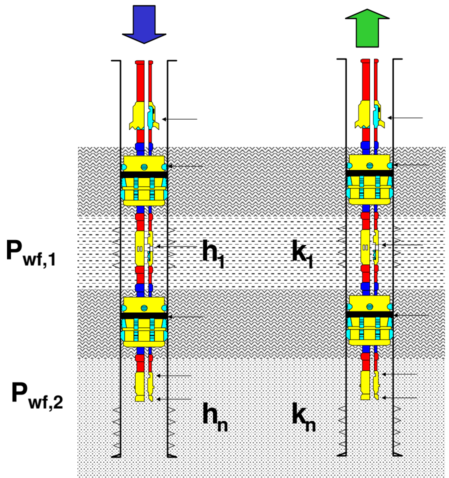

Figure 1: Well configuration for a two-layered reservoir with downhole pressure sensors

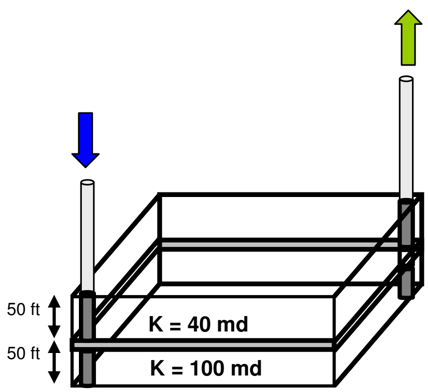

Figure 2: Reservoir configuration for a two-layered reservoir with one producer and one injector

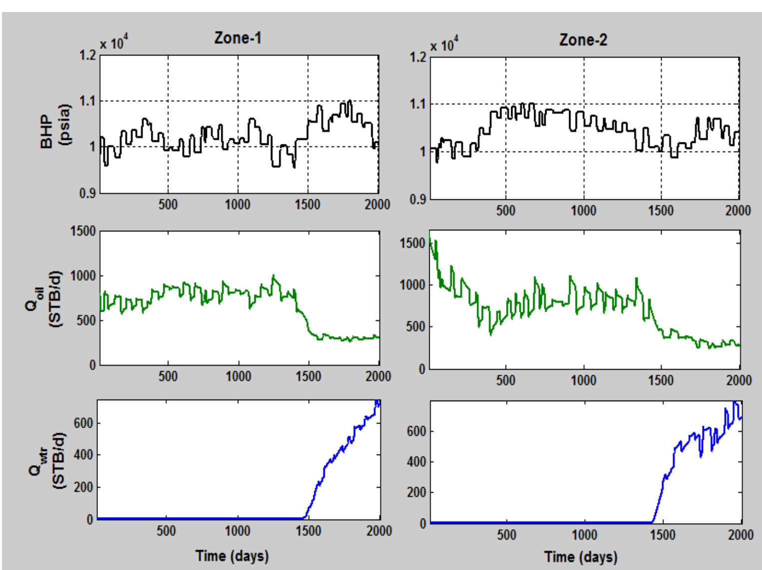

Figure 3: Zonal production data for the injector/producer example in Figure 2

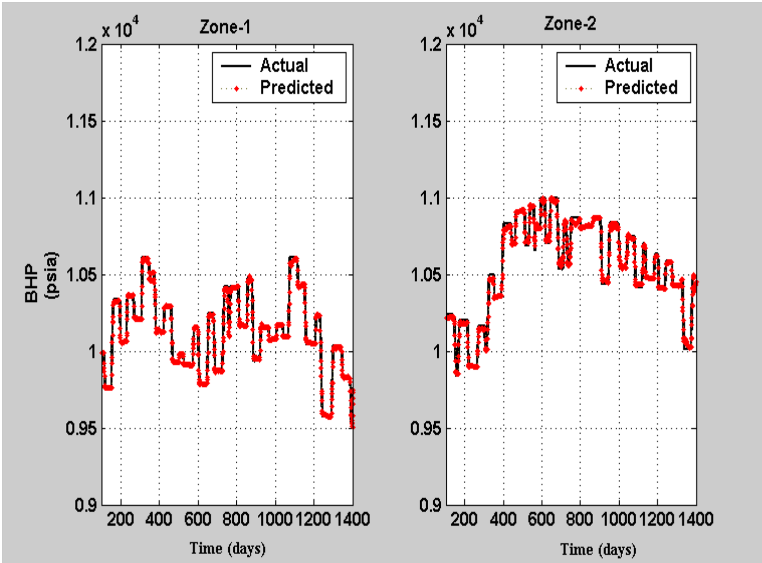

Figure 4: Comparison of actual and 7-day-ahead prediction of the bottomhole pressures (Zone-1 and Zone-2) for injector/producer example in Figure 2

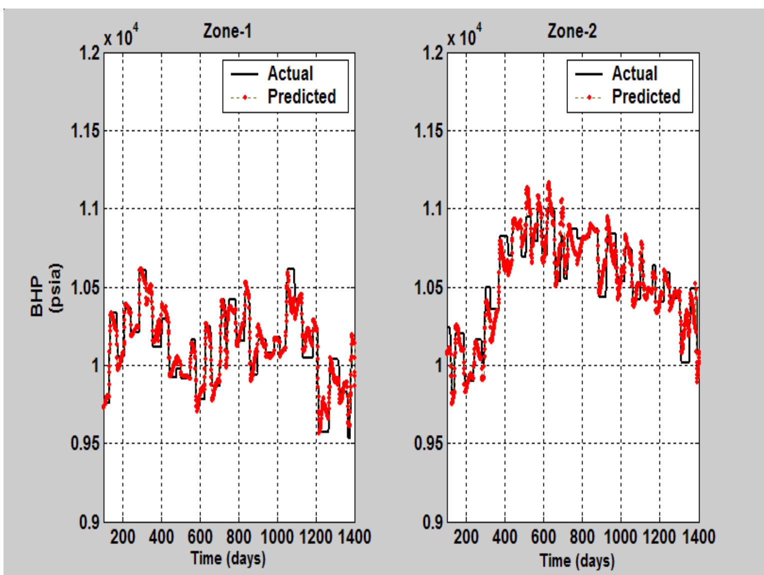

Figure 5: Comparison of actual and 30-day-ahead prediction of the bottomhole pressures (Zone-1 and Zone-2) for injector/producer example in Figure 2

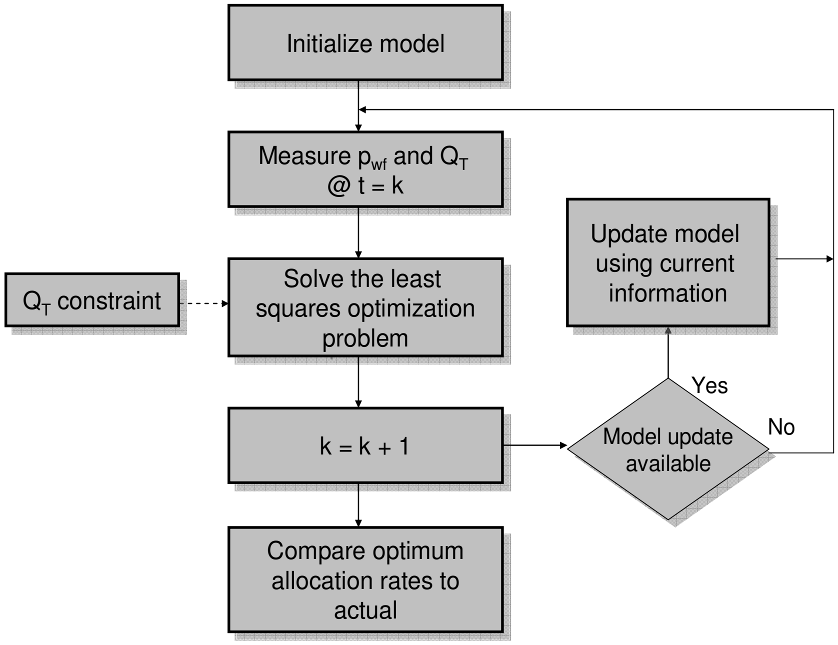

Figure 6: Production allocation workflow

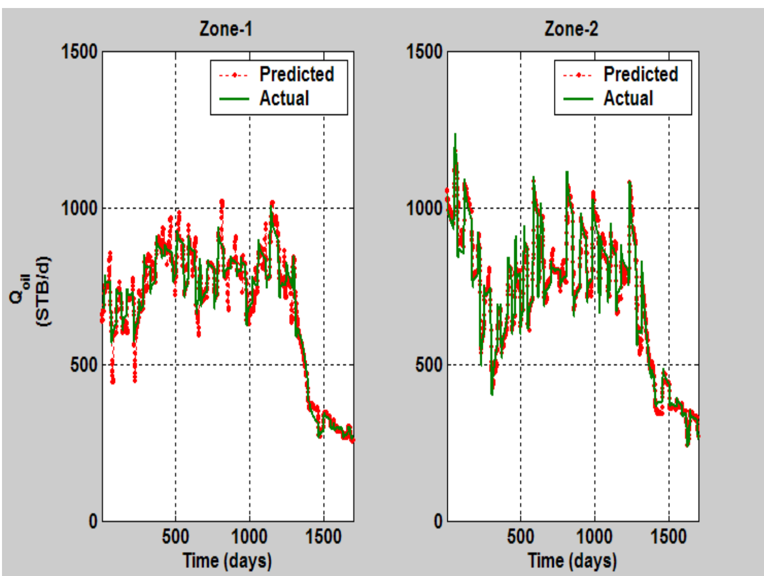

Figure 7: Case study I – Comparison between the optimal allocated (predicted) oil rates and the actual rates for both the zones with the model updated every 30 days

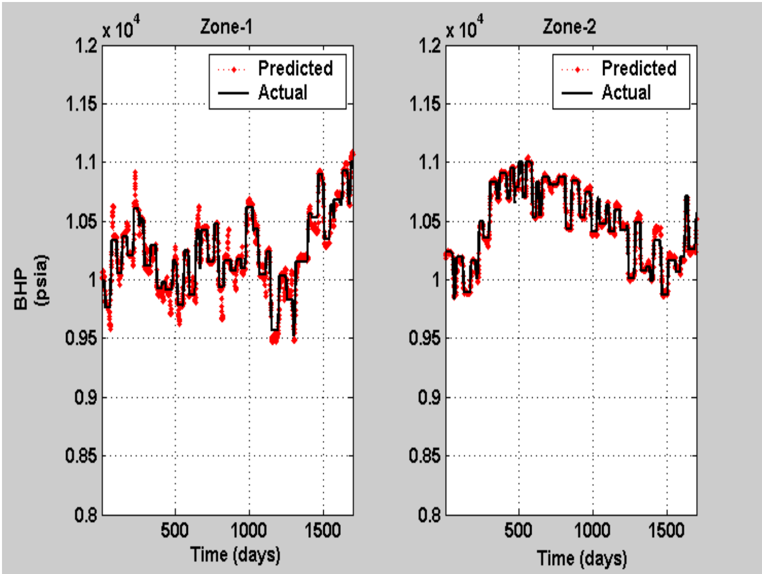

Figure 8: Case study I – Comparison between the predicted bottomhole pressures and the actual (measured) pressure while the model is updated every month

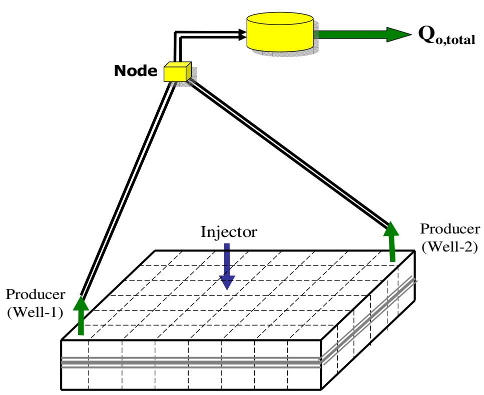

Figure 9: A simple schematic of a two layered reservoir with two producers and one injector connected to the production separator (at the surface network) through pipes

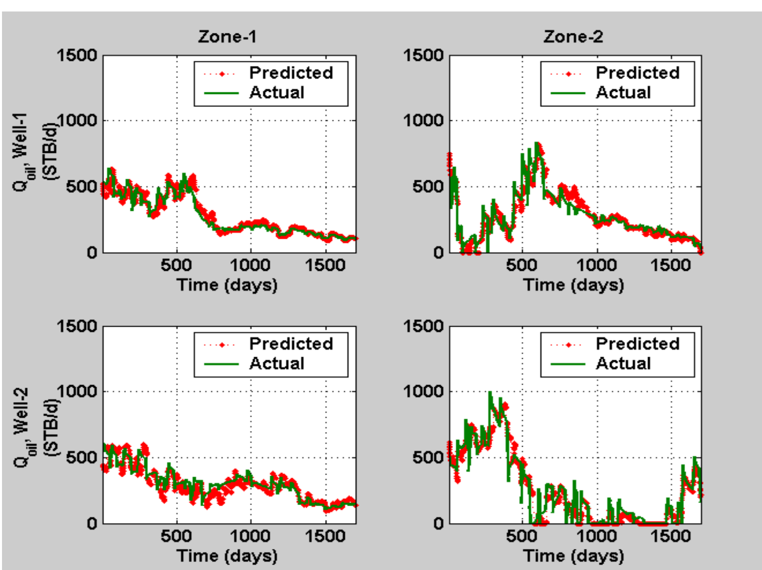

Figure 10: Case Study II - Comparison between the optimal allocated (predicted) oil rates and the actual rates for the two producers and their respective zones

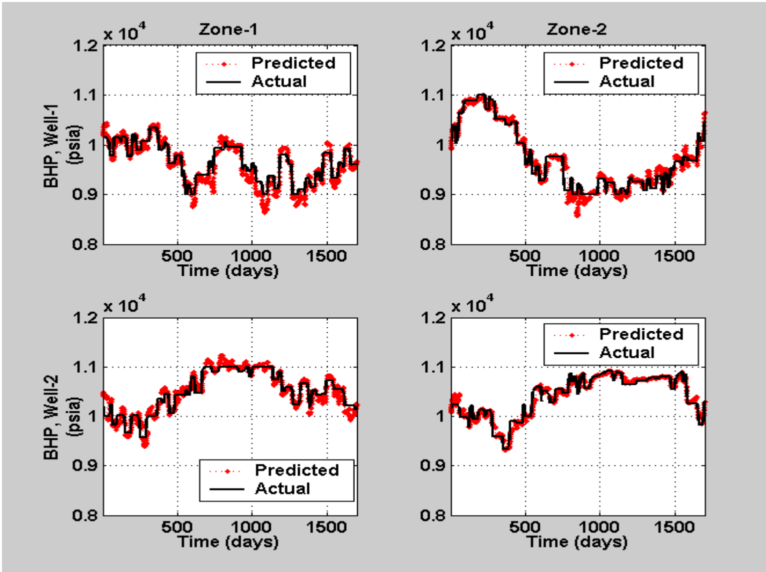

Figure 11: Case Study II – Comparison between the predicted bottomhole pressures and the actual (measured) pressure

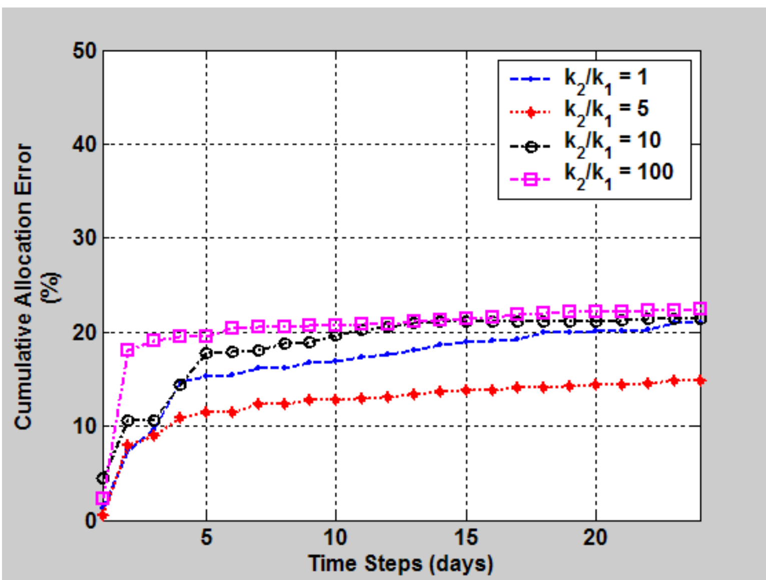

Figure 12: Cumulative allocation error (%) for different permeability ratios as a function of time (days)

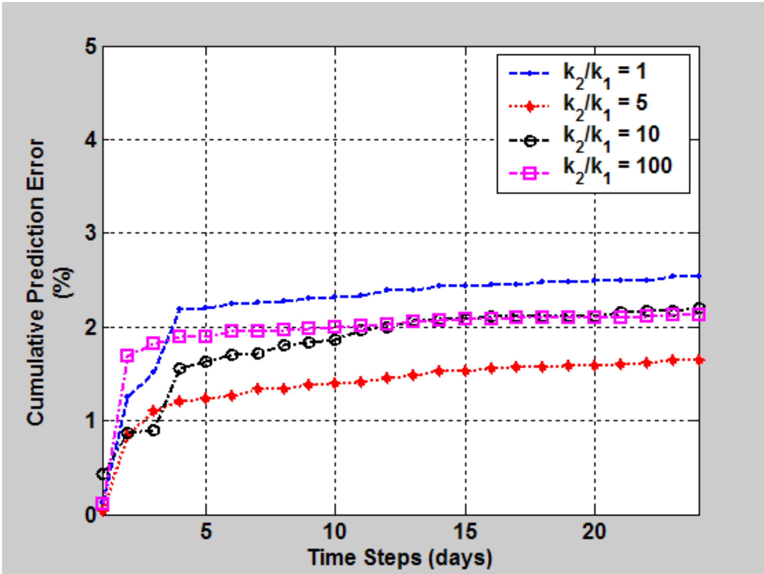

Figure 13: Cumulative prediction error (%) for different permeability ratios as a function of time (days)

Appendix A: Least Squares Optimization

Given the objective function in Eq. (3), minimizing deviation between the measured and the predicted output over a prediction horizon P:

$$J = [\sum_{j=1}^{P} (\hat{\mathbf{y}}_{k+j} - \mathbf{y}^m_{k+j})^T (\hat{\mathbf{y}}_{k+j} - \mathbf{y}^m_{k+j})] \tag{10}$$

$$\text{where } \hat{\mathbf{y}}_k = \begin{bmatrix} \hat{\mathbf{y}}_1 \\ \hat{\mathbf{y}}_2 \\ \cdot \\ \cdot \\ \hat{\mathbf{y}}_{N_z} \end{bmatrix}_k \text{ and } \hat{\mathbf{y}}^m_k = \begin{bmatrix} \hat{\mathbf{y}}^m_1 \\ \hat{\mathbf{y}}^m_2 \\ \cdot \\ \cdot \\ \hat{\mathbf{y}}^m_{N_z} \end{bmatrix}_k \tag{11}$$

The objective function can be re-written as:

$$J = (\hat{\mathbf{Y}} - \mathbf{Y}^m)^T (\hat{\mathbf{Y}} - \mathbf{Y}^m) \tag{12}$$

$$\text{where } \hat{\mathbf{Y}} - \mathbf{Y}^m = \begin{bmatrix} (\hat{\mathbf{y}}_k - \mathbf{y}^m_k) \\ (\hat{\mathbf{y}}_{k+1} - \mathbf{y}^m_{k+1}) \\ \cdot \\ \cdot \\ (\hat{\mathbf{y}}_{k+P-1} - \mathbf{y}^m_{k+P-1}) \end{bmatrix} \tag{13}$$

Using the parametric model in Eq. (2) to predict in the future, it can be shown that

$$\hat{\mathbf{Y}} = \mathbf{P}_1 \mathbf{x}_k + \mathbf{P}_2 \mathbf{u}^P \tag{14}$$

$$\text{where } \mathbf{P_1} = \begin{bmatrix} \mathbf{C} \\ \mathbf{CA} \\ \mathbf{CA}^2 \\ \cdot \\ \cdot \\ \mathbf{CA}^{P-1} \end{bmatrix}, \ \mathbf{P}_2 = \begin{bmatrix} \mathbf{D} & \cdot & \cdot & \mathbf{0} \\ \mathbf{CB} & \mathbf{D} & \cdot & \mathbf{0} \\ \mathbf{CAB} & \mathbf{CB} & \mathbf{D} & \mathbf{0} \\ \cdot & \cdot & \cdot & \cdot \\ \cdot & \cdot & \cdot & \cdot \\ \mathbf{CA^P B} & \mathbf{CA^{P\text{-}1} B} & \cdot & \mathbf{CA^{P\text{-}M} B + D} \end{bmatrix} \text{ and } \mathbf{u}^P = \begin{bmatrix} \mathbf{u}_k \\ \mathbf{u}_{k+1} \\ . \\ . \\ \mathbf{u}_{k+M-1} \end{bmatrix} \tag{15}$$

Combining Eq. (12) and Eq. (14), gives:

$$J = (\mathbf{u}^P)^T \mathbf{H} (\mathbf{u}^P) + 2(\mathbf{u}^P)^T \mathbf{f} \tag{16}$$

$$\text{where } \mathbf{H} = \mathbf{P}_2^T \mathbf{P}_2 \text{ and } \mathbf{f} = \mathbf{P}_2^T (\mathbf{P}_1 \mathbf{x}_k - \mathbf{Y}^m) \tag{17}$$

The equality constraint in Eq. (4), can be re-written in the following matrix form:

$$\mathbf{A}_e \mathbf{u}^P = \mathbf{b}_e \tag{18}$$

where $\mathbf{A}_e = \begin{pmatrix} \mathbf{I}_{N_z \times N_z} & & \\ & \text{O} & \\ & & \mathbf{I}_{N_z \times N_z} \end{pmatrix}$ and $\mathbf{b}_e = \begin{bmatrix} Q_{T,k} \\ Q_{T,k+1} \\ \cdot \\ \cdot \\ Q_{T,k+P-1} \end{bmatrix}$ (19)

The equality matrix $\mathbf{A}_e$ is a diagonal matrix, with each individual diagonal element an identity matrix of size $N_z \times N_z$, where N_z is the total number of zones.

Appendix B: Compact Parametric Model

The identified parametric model in Eq. (6) can be expanded for a given zone, i.e., $i = 1$:

$$\begin{aligned} \mathbf{x}_{k+1} &= \mathbf{A}_1 \mathbf{x}_k + \mathbf{B}_1 \mathbf{u}_k^1 \\ \hat{\mathbf{y}}_{k+1}^1 &= \mathbf{C}_1 \mathbf{x}_{k+1} + \mathbf{D}_1 \mathbf{u}_{k+1}^1 \end{aligned} \tag{20}$$

Similarly, expanding them for all the zones and combining all the state equations, as follows:

$$\mathbf{x}_{k+1} = \begin{pmatrix} \mathbf{A}_1 & & & & \\ & \mathbf{A}_2 & & & \\ & & \cdot & & \\ & & & \cdot & \\ & & & & \mathbf{A}_{N_z} \end{pmatrix} \mathbf{x}_k + \begin{pmatrix} \mathbf{B}_1 & & & & \\ & \mathbf{B}_2 & & & \\ & & \cdot & & \\ & & & \cdot & \\ & & & & \mathbf{B}_{N_z} \end{pmatrix} \begin{bmatrix} \mathbf{u}_{k+1}^1 \\ \mathbf{u}_{k+1}^2 \\ \cdot \\ \cdot \\ \mathbf{u}_{k+1}^{N_z} \end{bmatrix} \tag{21}$$

It should be noted that the dimension of the state vector ($\mathbf{x}$) in Eq. (20) is determined by the order n_i of the model, while the state vector ($\mathbf{x}$) in Eq. (21) has the order n :

$$n = \sum_{i}^{N_z} n_i \tag{22}$$

Similarly, the output equation can be combined as follows:

$$\hat{\mathbf{y}}_{k+1} = \begin{bmatrix} \hat{\mathbf{y}}_{k+1}^1 \\ \hat{\mathbf{y}}_{k+1}^2 \\ \cdot \\ \cdot \\ \hat{\mathbf{y}}_{k+1}^{N_z} \end{bmatrix} = \begin{pmatrix} \mathbf{C}_1 & & & & \\ & \mathbf{C}_2 & & & \\ & & \cdot & & \\ & & & \cdot & \\ & & & & \mathbf{C}_{N_z} \end{pmatrix} \mathbf{x}_k + \begin{pmatrix} \mathbf{D}_1 & & & & \\ & \mathbf{D}_2 & & & \\ & & \cdot & & \\ & & & \cdot & \\ & & & & \mathbf{D}_{N_z} \end{pmatrix} \begin{bmatrix} \mathbf{u}_{k+1}^1 \\ \mathbf{u}_{k+1}^2 \\ \cdot \\ \cdot \\ \mathbf{u}_{k+1}^{N_z} \end{bmatrix} \tag{23}$$